

Electrosynthesis of Ferrate (VI) ion Using High Purity Iron Electrodes: Optimization of Influencing Parameters on the Process and Investigating Its Stability

Sibel Barışçı^{1,*}, Feride Ulu¹, Heikki Särkkä², Anatholy Dimoglo¹ and Mika Sillanpää²

¹ Gebze Institute of Technology, Environmental Engineering Department, 41400, Gebze, Kocaeli, Turkey

² Lappeenranta University of Technology, LUT Savo Sustainable Technologies, Laboratory of Green Chemistry, Sammonkatu 12, FI-50130, Mikkeli, Finland

*E-mail: sbarisci@gyte.edu.tr

Received: 13 December 2013 / *Accepted:* 16 January 2014 / *Published:* 23 March 2014

This study is focused on the determination of optimum conditions for ferrate (VI) production and its stability. The effect of various operating parameters, such as NaOH concentration, current density, temperature and electrolysis duration on the yield of electrochemical ferrate (VI) ion production was investigated for high purity iron electrodes. Cyclic Voltammetry (CV) studies were carried out to characterize a process that takes place on the working iron electrode. The surface of high purity iron electrode was analyzed by Scanning Electron Microscopy (SEM). Electrosynthesized ferrate (VI) ion stability at different conditions was also investigated. Factors influencing the stability were initial ferrate (VI) ion concentration, alkalinity, temperature, and pH of the solution. Ferrate (VI) ion showed high stability at higher alkalinity, lower temperatures, increasing ferrate (VI) ion concentration and pH in the range between 9.2 and 10. Current efficiency and energy consumption were used for the optimum parameters determination for the ferrate (VI) production. According to the experiments, the optimum conditions were NaOH (as anolyte) concentration of 20 M, current density of 1.47 mA/cm², and temperature of 30 ± 1 °C with electrolysis duration of 1.5 hours. Ferrate (VI) ion solutions with contents up to 2.0 mM were produced in the electrochemical cell.

Keywords: Ferrate (VI), electrochemical synthesis, green oxidant, optimum conditions, stability.

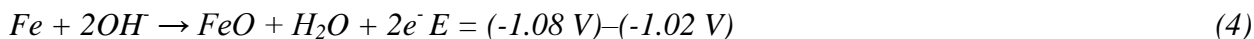
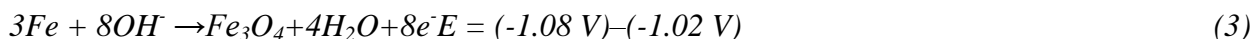
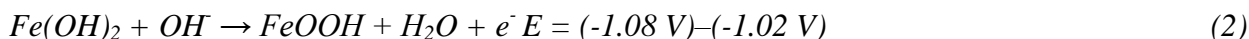
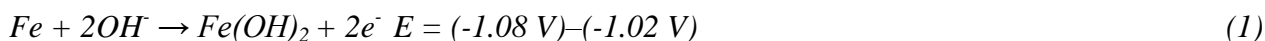
1. INTRODUCTION

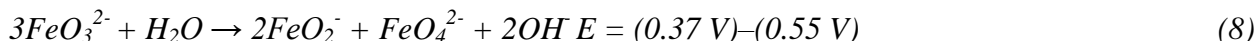
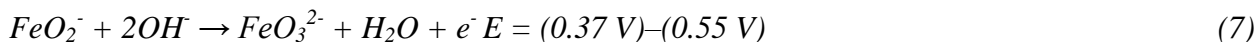
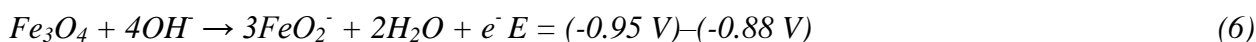
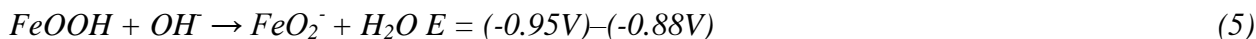
Over the last twenty years considerable attention has been focused on the elimination of pollutants through reactions activated by non-traditional methods. Electrochemical methods such as

direct oxidation, indirect oxidation and electrochemically produced oxidants have been demonstrated to be effective on a number of organic pollutants dissolved in water [1-3]. Electrochemical direct current and alternating current techniques were found to be suitable for metal dissolution studies in both aqueous and molten environments [4-6].

Hexavalent iron species, commonly known as ferrate, has been known for over a century, but its keystones are still being investigated and discovered [7, 8]. Ferrate species have the reduction potentials of 2.20 V at acidic conditions and 0.72 V at alkaline conditions. During the oxidation of pollutants, ferrate (VI) is reduced to a non-toxic byproduct, Fe (III), which is a well-known coagulant in the water and wastewater treatment. Therefore, ferrate (VI) is one of the most powerful, multipurpose, environmentally friendly water and wastewater treatment chemicals. For this reason, there is now an increasing interest in the use of innovative aqua ferrate (VI) technology in oxidizing emerging contaminants, toxic substances and deactivating microorganisms that have detrimental effects on human body in water and wastewater treatment without generating harmful by-products [9-15]. In a single dose, super-charged iron (6+) replaces multiple treatment chemicals, because it can simultaneously oxidize, disinfect and coagulate to remove pathogens and contaminants from water and wastewater. Because of these unique properties of ferrate (VI), its preparation methods have been considered for many years by different researchers [16-19]. Ferrate (VI) production methods can be divided into three main categories: (i) wet chemical synthesis, (ii) dry chemical synthesis and (iii) electrochemical synthesis. Among these methods, the electrochemical method has such advantages as simplicity, safety, and the absence of hypochlorite. The electrochemical method is also more cost effective process than other methods, as it does not require expensive chemicals.

Ferrate (VI) can be synthesized electrochemically by using either a dissolving iron anode in highly alkaline media or an inert electrode in Fe (III) solution. The first process of electrochemical production of ferrate (VI) mentioned consists of a sacrificial iron anode in an electrolysis cell containing highly strong alkaline media with a current serving to oxidize iron to Fe⁶⁺. Different mechanisms have been proposed to explain the process of the ferrate (VI) formation in the electrochemical cell. The three-step mechanism based on the intermediates formation can be proposed as the formation of intermediate species, the formation of ferrate and the passivation of the electrode. The formation of passive layer prevents further ferrate generation [20, 21]. The equations below show iron behavior in highly alkaline media; primarily, active dissolution of iron, and surface layer restructuring take place according to eq. 1, 2, 3 and 4. Then, it is assumed that the solid oxides and hydroxides formed on the surface of the anode are dissolved in the interaction with the hydroxyl ions that breaks down the iron surface and enables continuous dissolution of the anode (eq. 5, 6). Passivity and, subsequently, an intensive reaction of oxygen evolution overlapping the transpassive iron dissolution including ferrate (VI) formation pass according to reactions from eq. 7, 8 and 9. The potential regions depend on the electrolysis conditions and composition of materials [22-24].





The method of electrochemical synthesis of ferrate (VI) has been recently developed by anodic dissolution of iron in transpassive region in highly alkaline solvents [25]. During the anodic dissolution of iron in transpassive region, the surface of the anode becomes increasingly covered with iron oxide/hydroxide species. The local deterioration of the passive layer and formation of a porous oxide-hydroxide layer enhance ferrate formation at potentials close to the potential of competing oxygen evolution. The Fe (V) formation goes through the reaction with the Fe (III) and Fe (VI) participation. The efficiency of synthesis depends on the resistance of the oxide-hydroxide layer and the synthesis conditions, namely, electrolyte composition, electrode composition, and the temperature at which the synthesis is done.

The electrochemical production of ferrate (VI) can be remarkably affected by many factors, predominantly, current density [26-28], the electrolyte type and concentration [18], anode composition [18, 29] and temperature [18]. It was reported that the optimum NaOH concentration for the ferrate synthesis is in the range of 10–14 M [22, 30]. However, some researchers have found that 16 M NaOH media gave the best performance for ferrate (VI) synthesis [20, 30]. Alsheyab et. al. [31] also indicated that 20 M NaOH media showed high efficiency as well. Through the detailed analysis of the impact of NaOH, KOH and LiOH on the ferrate synthesis at various temperatures (20 °C, 30 °C and 40 °C), NaOH was shown to be the most promising option that provides the highest current yields [22]. This is caused by the individual products (FeO_4^{2-} and its intermediates) solubility in the process of electrolysis and the impact of individual cations on the structure of the surface layers, so as on their protective properties. In summary, several attempts have been made to commercialize ferrate (VI) synthesis, but this method is not completely developed. Further works on the process are needed to find out optimum synthesis conditions before a breakthrough can be obtained for real scale applications.

The stability of ferrate (VI) is also very important characteristic, when the potential practical synthesis and use of ferrate (VI) are considered. Due to its strong oxidizing properties, ferrate (VI) is relatively unstable in the presence of water [32]. It undergoes rapid decomposition according to eq. (10):



The decomposition rate of ferrate (VI) depends strongly on the initial ferrate concentration, alkalinity, temperature, pH and co-existing ions [33]. A full understanding of the effect of these factors on the stability and reactivity of electrogenerated ferrate (VI) solutions is essential prerequisite for the efficient use of ferrate (VI) solutions in water and wastewater treatment processes. The stability of solid ferrate (VI) in aqueous solutions has been investigated so far by many researchers [34-36], but nonetheless the stability of electrogenerated ferrate (VI) has not been researched. In this paper, our aim

is to investigate the stability of ferrate (VI), which is produced by the electrochemical method, and to gain information on the stability and the storage of electrosynthesized ferrate (VI), which is currently missing in the literature. This paper presents new information concerning the stability of electrogenerated ferrate (VI) and the factors that influence the process.

One of the purposes of this paper is to define optimum operating conditions for the electrochemical ferrate (VI) production which can be used for pilot scale plants. High purity iron plates as electrodes and NaOH as anolyte were investigated. NaOH concentration, current density and temperature were taken as three main parameters that influence ferrate (VI) production in an electrochemical cell. Stability studies were also conducted as the other objective of this paper. Effect of electrolyte type, alkalinity, initial concentration of ferrate (VI), temperature and pH were used to analyze the stability of the electrogenerated ferrate (VI). This is the first paper that investigates the stability of electrosynthesized ferrate (VI).

2. EXPERIMENTAL SECTION

2.1 Chemicals

Chemicals for ferrate (VI) measurements were analytical grade and used without further purification. Potassium ferrate (K_2FeO_4 , purity of 97%), sodium hydroxide (pellets, anhydrous, purity of $\geq 98\%$) and potassium hydroxide (pellets, purity of $\geq 85\%$) were supplied by Sigma Aldrich. pH values of ferrate (VI) solutions for the stability studies were controlled with buffer solutions. The buffers used in this study included: $C_8H_5KO_4$ -NaOH solution (pH 5.0), KH_2PO_4 -NaOH solution (pH 6.0, 7.0 and 8.0), $Na_2B_4O_7 \cdot 10H_2O$ -NaOH solution (pH 9.2 and 10.0), K_2HPO_4 -NaOH solution (pH 11.0). All solutions were prepared with high quality pure water using Millipore Water Purification System.

2.2 Analytical Procedures and Quantification for Ferrate (VI)

The concentration of ferrate (VI) was analyzed by Perkin Elmer Lambda 45 UV/VIS Spectrophotometer. It should be noted that UV spectrum has been obtained for the electrosynthesized FeO_4^{2-} as well. It is identical to the spectrum of potassium ferrate salt (with the maximum absorbance reached under 505 nm). This allowed for the further determination of the FeO_4^{2-} concentration with high accuracy.

Calibration curves for each NaOH concentration were prepared in accordance with the planned experiments. For this purpose, NaOH solutions of different concentrations (5 M, 10 M; 12 M; 14 M, 16 M and 20 M) were prepared, and different amounts of potassium ferrate were added to these solutions. So that 0.10;0.20; 0.25; 0.5; 1.0; 1.5; 2; 2.5 mM potassium ferrate solutions in alkaline media were gained. Their absorbance was measured at $\lambda = 505$ nm. R^2 values of calibration curves were greater than 0.99. This procedure was conducted without preparing stock solution because of

instability of solid potassium ferrate. For this reason, desired amount of potassium ferrate was weighed and added to each NaOH solution separately and analyzed immediately.

To use the established method and to keep an additional check on the accuracy and precision of the method, the recovery studies were conducted by addition of known amount of potassium ferrate or its solutions to pre-analyzed solutions in a wide concentration range, from 0.05 to 5 mM. Standard deviations and standard errors were also calculated. The mean recoveries of ferrate (VI) for various ferrate (VI) concentrations can be seen in Table 1. The established method showed good recoveries of ferrate (VI) and was found to be satisfactory.

Table 1. Recoveries of ferrate (VI) with different concentrations.

Ferrate (VI) Conc. (mM)	n	Recovery (%)	Mean Recovery (%)	Standard Deviation	Standard Error
0.05	5	88-111	99.08	0.084	0.038
0.1	5	88-116	102.25	0.204	0.091
0.25	5	92-103.5	98.9	0.094	0.042
0.5	5	95-110.8	100.9	0.049	0.022
1	5	100.9-110.1	102.2	0.193	0.086
5	5	98.8-106	102.4	0.441	0.197

2.3 Electrode Material

High purity iron plate electrodes were supplied by Artı Makina, Turkey. The electrodes were suitable for the EN 10025-2 standards. Chemical composition of the electrodes is shown in Table 2. As it is seen in Table 2, the iron content of the electrodes was 99.195%.

Table 2. Chemical composition of high purity iron electrodes used in the experiments (in percent).

C	Mn	Si	P	S	Cr	Ni	Cu	Al	Mo	V
0.07	0.59	0.01	0.01	0.005	0.03	0.04	0.01	0.033	0.003	0.004

Dimensions of the electrodes were 10 x 5 x 0.2 cm. The electrodes were connected by iron rods and squeezed by screws and seal rings to be fixed to the electrochemical cell.

2.4 Voltammetry Studies

Cyclic voltammetry (CV) experiments were performed using an advanced electrochemical system, a computer-controlled potentiostat-galvanostat Princeton Applied Research Parstat 2273. The working electrode was iron wire with the area of 0.32 cm². The counter electrode was Pt wire, where Ag|AgCl was used as a reference electrode. The electrode potentials were measured in three-electrode

cylindrical glass cell filled with different concentrations of NaOH (5, 12, 16 and 20 M). The experiments were conducted at 30 ± 1 °C. Cyclic voltammograms were recorded at scan rate of 10 mV/s. Before each analysis, the impurities on the iron wire electrode surface were removed by emery paper.

2.5 Scanning Electron Microscopy

The surface of a high purity iron electrodes was examined before and after the electrolysis by Hitachi S4800 scanning electron microscope (SEM) operated at 30 kV.

2.6 Electrochemical Run

The electrosynthesis was carried out in a plexiglass electrochemical cell. The dimensions of the cell were 12 x 7 x 5 cm, and the wall thickness was 0.2 cm. Two anodes and two cathodes which were connected as monopolar position were used for each experiment. Prior to the electrolysis, electrodes were washed with 0.5 N H₂SO₄ solution for 2 minutes and rinsed with deionized water, then they were dried in the oven and placed in a desiccator to cool down. The same procedure was applied as well as after each experiment. Then the electrodes were weighed before and after each experiment to find out amount of dissolved iron. The value was used for the calculation of amount of ferrate (VI) obtained experimentally. As it is seen, in eq. (11) current efficiency (CE) was calculated being based on the ratio of the experimentally synthesized ferrate (VI), $[\text{FeO}_4^{2-}]_e$, to the theoretical amount of ferrate (VI), $[\text{FeO}_4^{2-}]_t$, according to the Faraday's Law (Eq. 12).

$$\text{Current Efficiency (CE)} = [\text{FeO}_4^{2-}]_e / [\text{FeO}_4^{2-}]_t \times 100 (\%) \quad (11)$$

$$[\text{FeO}_4^{2-}]_t = M_w I t / z F \quad (12)$$

Where M_w is the molecular weight of ferrate (VI) (120 g/mol); I is applied current (A); t is electrolysis time (sec.); z is number of electrons involved to the reaction (6); F is Faraday's Law constant (96485 Coulomb/mol).

In other respects, energy consumption is one of the most important factors for a process to be cost effective. It has to be taken into account for establishing industrial scale processes. Hence, it was calculated using the following eq. (13), which mostly depends on the cell voltage of the electrochemical process.

$$\text{Energy Consumption (EC)} (\text{kWh/kg}) = V I t / m \quad (13)$$

Where V is the cell voltage (V); I is the applied current (A); t is the electrosynthesis time (h); m is the amount of ferrate (VI) gained (kg).

Constant direct current was supplied by GW Instek PSP-405 Programmable DC power source. The cell voltage was recorded during the electrosynthesis. Electrolyte was stirred by magnetic stirrer. Temperature and pH were controlled by WTW Inolab Multi 9310 IDS pHmeter. Electrolysis duration was 1.5 hours. Samples were taken from the electrochemical cell and analyzed by UV/VIS spectrophotometer immediately. Measurements were duplicated, and their average was taken. Experiments were conducted at 20 ± 1 , 30 ± 1 , 50 ± 1 and 65 ± 1 °C, which was supplied by water bath, to determine effect of temperature on the ferrate (VI) yield. The experiments were also conducted with different alkaline concentrations, as mentioned in the second paragraph of the material and methods section, to indicate the effect of NaOH concentration on the ferrate (VI) yield.

The active total surface area (S_{total}) of the electrodes was 81.25 cm^2 . Current densities were calculated for each applied current by dividing the applied current by S_{total} . Different current densities (1.47 , 3.08 and 4.55 mA/cm^2) were applied to see the effect.

The optimum conditions were determined in terms of current efficiency (CE), energy consumption (EC) and amount of ferrate (VI) produced.

2.7 The Stability of Electrosynthesized Ferrate (VI)

The stability of electrosynthesized ferrate (VI) in terms of type of electrolyte, initial ferrate (VI) concentration, temperature, alkalinity and pH was examined.

This part of the study was conducted producing ferrate (VI) by electrochemical way in different electrolyte media such as NaOH, KOH and NaOH/KOH mixture solutions for investigating the effect of electrolyte type on the stability. Experiment conditions were chosen as electrolyte concentration of 20 M and current density of 1.47 A/m^2 . Initial ferrate (VI) concentration was 1.65 M for each media. Before the experiments, calibration curves established for 20 M NaOH, KOH and NaOH/KOH mixture separately for ferrate (VI) measurement.

To study the effect of the initial ferrate (VI) concentration on its stability, three different concentrations (0.773 , 1.05 and 1.65 mM) obtained from the experiment with 20 M NaOH media, and $I_d = 1.47 \text{ mA/cm}^2$ at the temperature of 30 ± 1 °C were used.

To assess the effect of temperature, ferrate (VI) was generated in 20 M NaOH media with the current density of 1.47 mA/cm^2 at 30 ± 1 °C, electrolysis duration of 1.5 h and then placed in a water bath to reach the desired final temperatures. Ferrate (VI) concentration was reduced by approximately 5% before reaching the final temperatures. Thus, the initial ferrate (VI) concentration was $1.65 \pm 0.01 \text{ mM}$, and the studied temperatures were $+4$, $+20$, $+30$ and $+50$ °C.

The dependency of ferrate (VI) stability on different NaOH concentrations was investigated for its 5, 10, 12, 14, 16 M and 20 M solutions. The initial concentration of ferrate (VI) was $0.35 \pm 0.01 \text{ mM}$ for each NaOH media. This concentration was different from other studies because low ferrate (VI) quantity was achieved for low NaOH concentrations such as 5 and 10 M. To determine the effect of alkalinity, accurate concentrations should be provided. Therefore, $0.35 \pm 0.01 \text{ mM}$ was chosen as initial ferrate (VI) concentration for investigating the effect of alkalinity.

Wavelength scan in the range of $\lambda = 450\text{-}600$ nm was conducted for the ferrate (VI) solutions every 10 minutes during 1 hour, and decreasing absorbance values at $\lambda = 505$ nm were recorded. Then ferrate (VI) concentrations were calculated according to the prepared calibration curves in advance for the studies explained above.

The pH-dependent decomposition of electrogenerated ferrate was determined in buffered solutions (as specified in the section of chemicals) by monitoring the temporal ferrate decrease in light absorbance at 505 nm every 30 seconds. For each experiment, initial ferrate concentration was 1.65 ± 0.01 mM, and the samples were immediately transferred to a 1 cm quartz cell for spectrophotometric determination of light absorbance. Investigated pH values were 5, 6, 7, 8, 9.2, 10 and 11. Characteristic kinetic plots ($[FeO_4^{2-}]$ vs. t ; $\ln[FeO_4^{2-}]$ vs. t ; $1/[FeO_4^{2-}]$ vs. t) were created for each pH value to determine the reaction order, and then kinetic constants were calculated according to the plots, which produced straight line.

3. RESULTS AND DISCUSSION

3.1 Characterization of Ferrate (VI)

Aqueous solution of ferrate ion has a characteristic purple-violet color, which corresponds to the visible and near-infrared absorption spectrum at about 450 and 600 nm. Figure 1 shows the UV/Vis absorption spectra for solid potassium ferrate and electrogenerated ferrate (VI) in 20 M NaOH solution. The spectra have the maximal absorption at the wavelength of 505 nm for both ferrate (VI) solutions. The absorption spectrum of potassium ferrate at 505 nm was confirmed by other studies [37, 38].

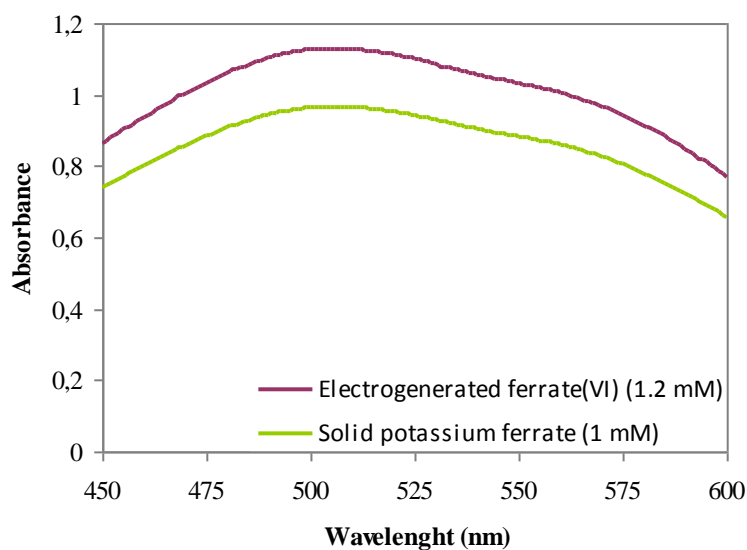


Figure 1. UV/Vis absorption spectrum of ferrate (VI) in 20 M NaOH media.

3.2 The Effect of the Parameters Selected on the Ferrate (VI) Yield

To get benefits from the superior performance of ferrate (VI) as an oxidant/coagulant/disinfectant for water and wastewater treatment in industrial scale and to prepare ferrate (VI) with high stability and low manufacturing cost as well, it is important to understand the mechanism and the properties of ferrate (VI). The following three main parameters were understood as crucial ones for the electrochemical synthesis of ferrate (VI).

3.2.1 Electrolyte Concentration and Current Density

One of the main factors that affect the electrochemical synthesis of ferrate (VI) is the composition of electrolyte and its concentration. The electrolyte type affects iron dissolution, the oxo-hydroxide layers covering the anode surface, and the solubility of the dissolution products. NaOH is the leading electrolyte for electrochemical preparation of ferrate (VI). However, there were different thoughts of researchers about the best electrolyte type for electrochemical ferrate (VI) synthesis. Many researchers have found that NaOH is more effective than KOH as an electrolyte [18, 27, 29, and 33]. On the other hand, some researchers reported that better results for the electrosynthesis were obtained with KOH [39]. In this study, the more commonly used NaOH was chosen as alkaline media.

Electrolyte concentration is as important as its type. For this reason, different concentrations of NaOH were studied. The dependence of ferrate (VI) yield on NaOH concentration for different current densities is shown in Figure 2. As it is seen in Figure 2, ferrate (VI) production increases with the increase of [OH⁻] ions concentration.

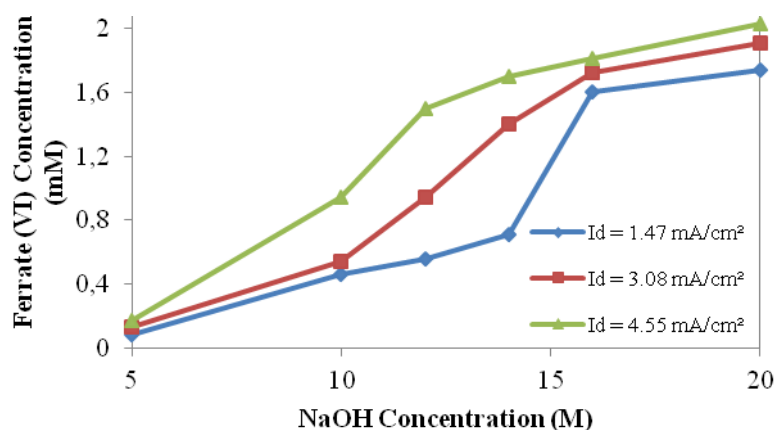
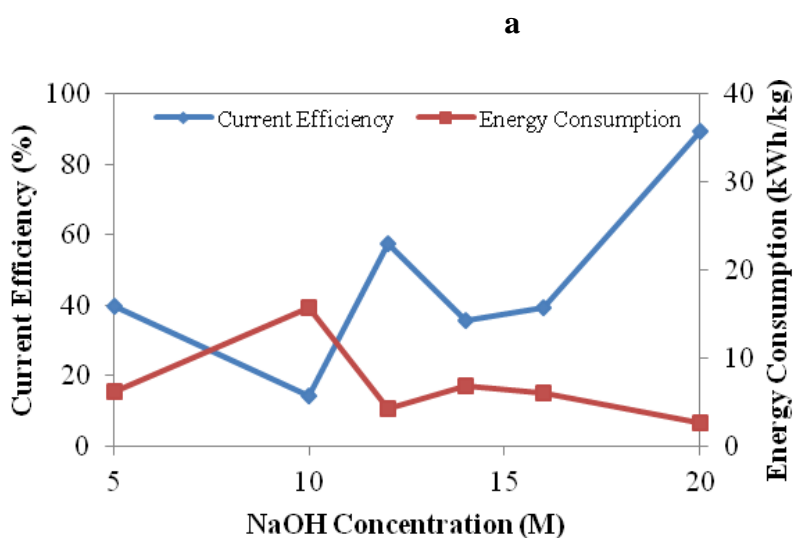


Figure 2. The effect of NaOH concentration in different current densities on ferrate (VI) produced in the electrochemical cell (electrolysis duration, 1.5 h; temperature, 30±1 °C.)

The maximum ferrate (VI) concentration (2.03 mM) was obtained in 20 M NaOH media with the current density of 4.55 mA/cm². Also, 1.91 and 1.74 mM ferrate (VI) in the same media with the current density of 3.08 mA/cm² and 1.47 mA/cm² produced in the electrochemical cell, respectively. This situation is a result of increasing alkalinity of anolyte increases the solubility of iron species with

lower valence. Also more concentrated anolyte media has a positive effect on iron dissolution and oxo-hydroxide layer covering the anode. The surface layer of anode resolves with more concentrated OH⁻ solutions and this increases iron dissolution and as well as ferrate (VI) stability.

Current density also affects the formation of ferrate (VI). When ferrate (VI) formation takes place in the anode surface with iron dissolution, it competes with the oxygen evolution. The increased potential causes higher involvement of this parasitic reaction which reduces the yield of ferrate (VI) [23, 40]. Also, it has been reported that the formation of hydrogen gas on the cathode increases as the current density increases, and this lowers the generated ferrate (VI) [41]. At the surface of electrodes, electric energy affects an electrochemical reaction followed by the formation of a gaseous phase, and a fraction of the solid surface covered by adhering bubbles lowers the transfer area [42]. According to the Figure 3, the results in 5, 12 and 20 M NaOH media were complied with this detection (the best result was at 1.47 mA/cm²). But, when the concentration of NaOH changed, the situation was different because of competing reactions in the electrochemical cell. The ferrate (VI) yield increased by 14.3%, 22.4% and 29.0% in 10 M NaOH media under increasing current density of 1.47, 3.08 and 4.55 mA/cm², respectively. At the same time, when current density for 14 M and 16 M NaOH concentrations increased from 1.47 to 3.08 mA/cm², the yield also showed increment with 46.0 % and 67.2 %, respectively. In contrast to this, the yield for 14 and 16 M NaOH media decreased with current density increasing from 3.08 to 4.55 mA/cm² by 19.3% and 26.6%, respectively. Under these circumstances, the whole mechanism (O₂ evolution, H₂ formation on cathode, anodic dissolution, and degradation of oxo-hydroxide layer) has to be considered together. The yield depends on the reaction which dominates in the media. Temperature and anode composition also determine the yield. Under normal operation of electrochemical reactors, small variations of current are reflected by small variations of potential. However, an enormous and often extraordinarily fast increase in potential can be observed, when under certain operation conditions a critical value of the current density is reached. The principal feature of this extraordinary operation condition is that the definite correlation between cell potential and cell current gets lost [43].



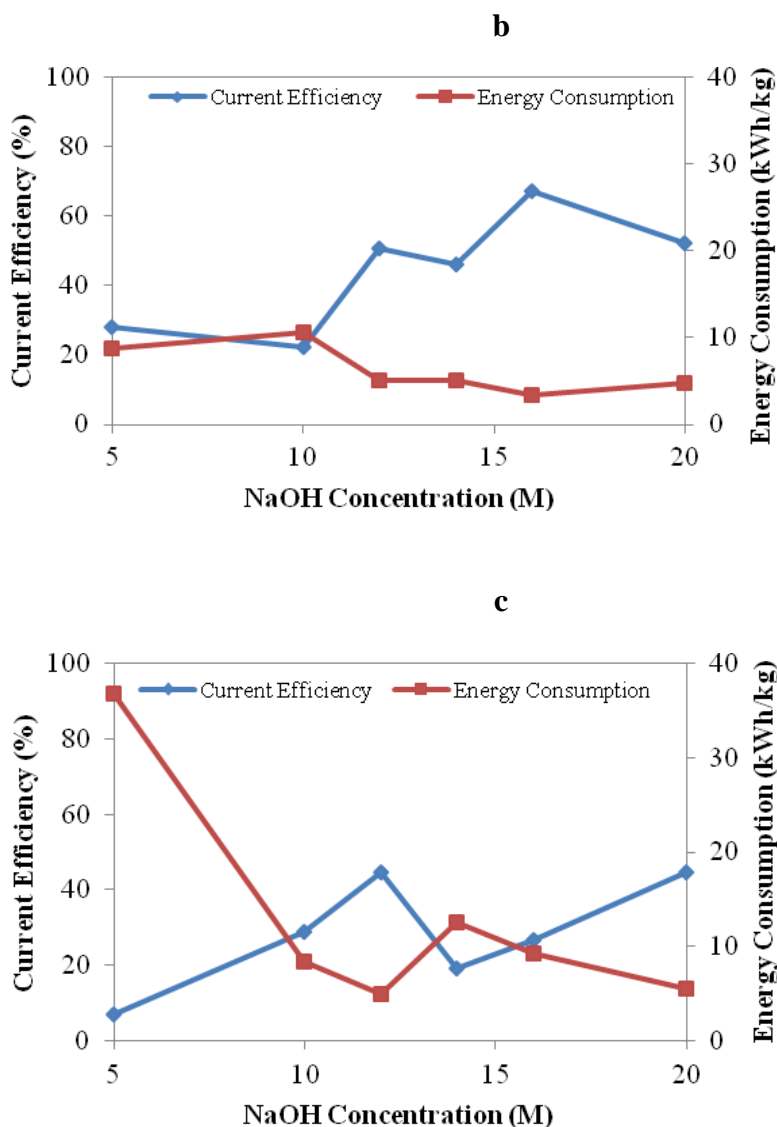


Figure 3. Current efficiencies and energy consumptions for different alkaline media; **a)** $I_d = 1.47 \text{ mA/cm}^2$, **b)** $I_d = 3.08 \text{ mA/cm}^2$, **c)** $I_d = 4.55 \text{ mA/cm}^2$ (electrolysis duration, 1.5 h; temperature, $30 \pm 1 \text{ }^\circ\text{C}$).

In this case, the effective current density was 1.47 mA/cm^2 for 5 M, 12 M and 20 M NaOH, 3.08 mA/cm^2 for 14 M and 16 M NaOH, and 4.55 mA/cm^2 for 10 M NaOH. In the overall assessment, the optimum conditions were 20 M NaOH media with the current density of 1.47 mA/cm^2 in terms of the highest current efficiency (89.5%) and the lowest energy consumption (2.616 kWh/kg).

3.2.2 Temperature

Temperature has a significant effect on the ferrate (VI) yield, but its effect depends on the anode material used. It was found that low temperature ($20 \text{ }^\circ\text{C}$) was better for white cast iron anode [20]. On the other hand, Ding et. al. [18] reported that higher efficiency was obtained by higher temperature for porous magnetite anode. In this study, temperatures of 20, 30, 50 and $65 \text{ }^\circ\text{C}$ were investigated for high purity iron anode. Obtained results are shown in Figure 4.

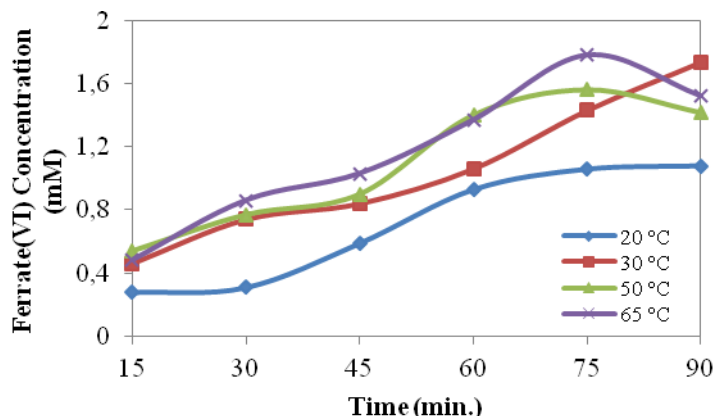


Figure 4. Effect of temperature on ferrate (VI) production rate (Ferrate (VI) was generated in 20 M NaOH with $I_d = 1.47 \text{ mA/cm}^2$ for each temperature).

According to Figure 4, while the highest production rate was obtained at 65 °C, the lowest production rate was at 20 °C after 75 min. electrolysis. 30 °C after 1.5 hours electrolysis time gave good result as well. It can be said that higher temperatures provide better production rates for high purity iron anodes. Electrolysis time is also important for determining the optimum temperature. Although higher production rate was obtained at 50 and 65 °C after the 75 min electrolysis, there was a drop after this time. Temperature has two main impacts on the ferrate (VI) yield. First, oxo-hydroxide layer occurring on the surface and causing the anode passivation degrades with the temperature increase. Thus, the surface of the anode material refreshes, and anodic dissolution and current yield tend to increase [39, 44]. Second, ferrate decomposition enhances with increasing temperature. To overcome this reverse effect, the limited product solubility in suitable anolyte solution of suitable concentration might be provided. It can be explained for this case that ferrate (VI) decomposition rate was greater than oxo-hydroxide layer disintegration after 75 min. for high purity iron electrodes with 20 M NaOH media.

3.3 Cyclic Voltammetry

Figure 5 shows the effect of NaOH concentration on the CV behavior of pure iron electrode at a scan rate of 10 mV/s using Ag|AgCl as a reference electrode. The formation of ferrate (VI) during the anodic scan is confirmed by the observation of a cathodic wave occurring at -0.25 V and this corresponds to the reduction of iron (VI) to iron (III). This result is in agreement with the previous researches [44-47]. There were no clear anodic or cathodic peaks for low NaOH concentration (5 M). Also, there were no such large anodic peaks during the scan for all concentrations. This can be related to the partial or whole overlap of anodic current peak corresponding to ferrate (VI) production with the current corresponding to oxygen evolution. On the other hand, the voltammetric charge of the cathodic peak for ferrate (VI) reduction shows its maximum value for the 20 M NaOH media. The latter was found as an optimum concentration for ferrate (VI) production. Also, the stability of the formed ferrate (VI) improves with the increase in the concentration of NaOH solution as will be indicated in the section on the self-decomposition of electrosynthesized ferrate (VI).

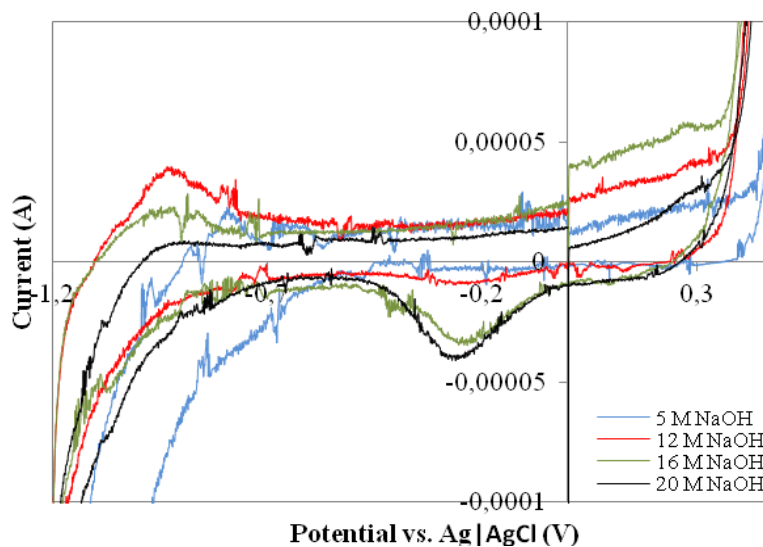


Figure 5. Cyclic voltammogram for high purity iron electrode in different NaOH concentrations at a scan rate of 10 mV/s and temperature of 30 ± 1 °C, potentials referred with respect to Ag|AgCl.

3.4 Surface Observations of Iron Anode

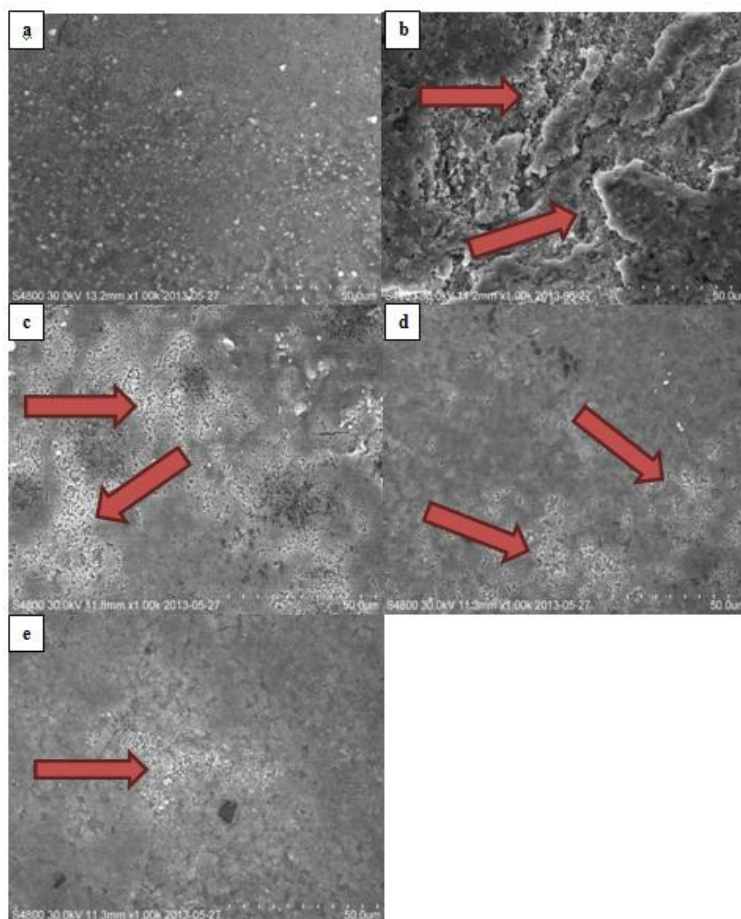
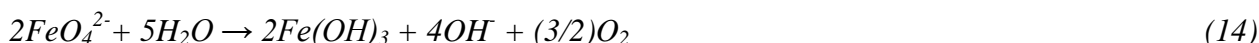


Figure 6. SEM photographs of high purity iron anodes **a)** in original state prior to electrolysis **b)** in 5 M NaOH media after electrolysis **c)** in 12 M NaOH media after electrolysis **d)** in 16 M NaOH media after electrolysis **e)** in 20 M NaOH media after electrolysis.

The scanning electron microscopy (SEM) was used to provide additional information about the mechanism that underlies the process. SEM observations (Figure 6.a) showed that the surface of the plate of high purity iron anode was highly smooth except for minor roughs. It can be seen in Figure 6.b that after whole experiments (4.5 hours electrolysis) in 5 M NaOH media, the surface of anode was covered with oxo-hydroxide layer, which has reverse effect on ferrate (VI) production rate and decreases the current efficiency, as mentioned before. Also, the decrease of this oxo-hydroxide layer with the increase of alkalinity of the solution can be seen in Figure 6 (c, d and e). These results are compatible with the data obtained in the experiments.

3.5 Self-Decomposition of Electrosynthesized Ferrate (VI)

The investigation of factors influencing stability of ferrate (VI) is essential as to estimating its potential use for the water and wastewater treatment applications. In general, ferrate (VI) ions, FeO_4^{2-} , decompose spontaneously with the following reaction (Eq. 14), i.e. the ferrate (VI) solution is unstable.



It has been reported that the self-decomposition rate of ferrate (VI) solution depends strongly on the initial ferrate (VI) concentration, pH of solutions, co-existing ions, alkalinity and temperature [48-50]. However, the stability of ferrate ions freshly produced by on-line electroynthesis has not been investigated, so far. Therefore, this section aims at evaluating the influence of type of electrolyte, initial ferrate concentration, alkalinity, temperature and pH on the freshly produced ferrate ions by electrochemical method.

3.5.1 Effect of Electrolyte Type

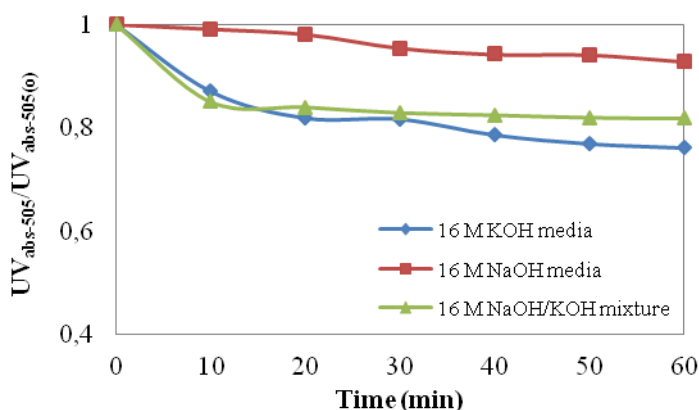


Figure 7. Effect of electrolyte type on the stability (Ferrate (VI) was generated in electrolyte concentration of 20 M, with $I_d = 1.47 \text{ mA/cm}^2$ at the temperature of $30 \pm 1 \text{ }^\circ\text{C}$ and initial ferrate (VI) concentration was 1.65 mM).

The stability of ferrate (VI) depends on the type of electrolyte. Experimental results showed that NaOH media was provided higher stability of electrosynthesized ferrate (VI) during time. In case of KOH solution, the decomposition ratio was almost 24% after one hour, while only 7% in NaOH

media. In case of the mixture of NaOH/KOH solution, the decomposition ratio was 18%. All the results can be seen in Figure 7. The results pointed out that NaOH was the most suitable electrolyte type for electrochemical production of ferrate (VI).

3.5.2 Effect of Initial Ferrate (VI) Concentration

The stability of ferrate (VI) is influenced by its initial concentration. Figure 8 illustrates the dependency of the electrogenerated ferrate (VI) stability on its concentration under 20 M NaOH media. In literature, diluted ferrate (VI) solutions were reported to be more stable than the concentrated ones for the aqueous ferrate solutions [32]. However, in our case, the ferrate stability decreased with decreasing ferrate concentration, which is reverse to that of ferrate in aqueous solution. As it is seen in Figure 8, the decomposition ratios were 8.2, 7.2 and 6.6% after 60 min. for the initial concentrations taken as 0.773, 1.05 and 1.65 mM, respectively.

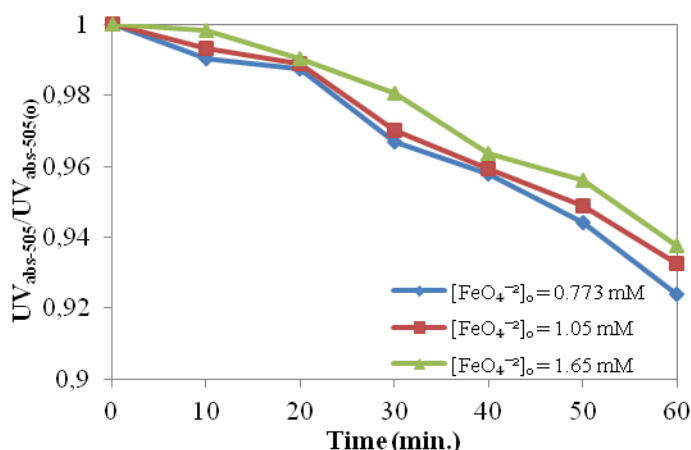


Figure 8. Effect of initial ferrate concentration on the stability (Ferrate (VI) was generated in 20 M NaOH media with $I_d = 1.47 \text{ mA/cm}^2$ at the temperature of $30 \pm 1 \text{ }^\circ\text{C}$).

3.5.3 Effect of Alkalinity

Alkalinity of the electrogenerated ferrate (VI) solution is one of the key factors of its stability. Figure 9 indicates that in 5 M NaOH media, ferrate (VI) decomposed by 29.3 % after 60 min. period, while in the case of 20 M NaOH media, the decomposition ratio was only 6.1% after the same period of time. The other decomposition ratios were 7.1, 10.6, 13.3 and 19.4% after 60 min period for 16, 14, 12 and 10 M NaOH media, respectively. Consequently, these results indicate that the stability of ferrate (VI) solution increases with increasing alkalinity.

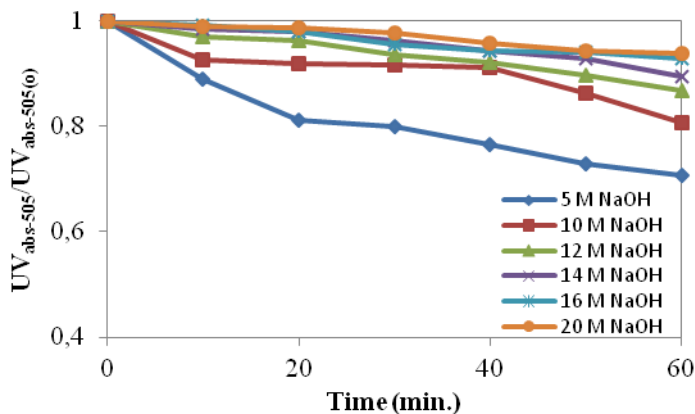


Figure 9. Effect of alkalinity of the solution on the stability (Ferrate (VI) was generated with $I_d = 1.47 \text{ mA/cm}^2$ for each NaOH media at the temperature of $30 \pm 1 \text{ }^\circ\text{C}$ and the initial ferrate (VI) concentration was $0.35 \pm 0.01 \text{ mM}$).

3.5.4 Effect of Temperature

Temperature is also one of the factors influencing the stability of electrogenerated ferrate (VI). Ferrate salts are unstable, particularly when stored at elevated temperatures [51]. According to the Figure 10, a stable period for the ferrate (VI) solution was observed at lower temperatures. At a constant temperature of $50 \text{ }^\circ\text{C}$, it was reduced by 35.3%, while at $4 \text{ }^\circ\text{C}$ for 1 h period it remained almost unchanged. Ferrate (VI) was almost stable for 1 h period (decomposition ratios were 4.9 and 6.3%) for the constant temperatures of $20 \text{ }^\circ\text{C}$ and $30 \text{ }^\circ\text{C}$, respectively.

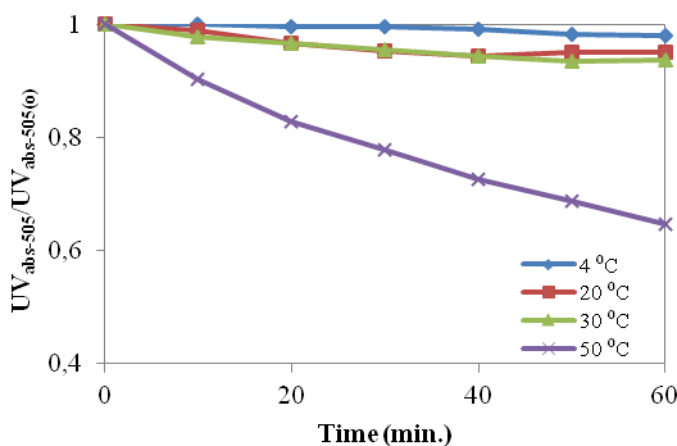


Figure 10. Effect of temperature of the solution on the ion stability (Ferrate (VI) was generated in 20 M NaOH media with $I_d = 1.47 \text{ mA/cm}^2$ at the temperature of $30 \pm 1 \text{ }^\circ\text{C}$, electrolysis duration, 1.5 h; initial ferrate concentration was $1.65 \pm 0.01 \text{ mM}$).

3.5.5 Effect of pH

The decomposition rate of ferrate (VI) depends on pH strongly. The spontaneous decomposition of ferrate was reported to be increased significantly with decreasing pH of the solution [35, 52].

It was found that self-decomposition of the electrosynthesized ferrate (VI) had second order reaction kinetics as indicated by some researchers: $-d[FeO_4^{2-}]/dt = k[FeO_4^{2-}]^2$ [53, 54]. The kinetic constant (k) was calculated for each pH. The experimental results are plotted in Figure 11. The decay kinetic constants shown graphically indicate that ferrate (VI) is more stable in the range of pH 9.2~10. Visually, decomposition of the electrosynthesized ferrate (VI) was accompanied by a remarkable change in the solution color. Initially, the ferrate (VI) solution was purple in color, and it rapidly became yellowish as decomposition occurred with decreasing pH. Finally the solution became colorless with some yellowish $Fe(OH)_3$ precipitates at the bottom of the beaker. It can be seen that under acidic conditions ferrate (VI) has a high oxidation potential that leads to rapid redox reactions causing the reduction of Fe (VI) to Fe (III). If $pH > 10$, it is believed that ferrate (VI) follows a different reduction pathway leading to the formation of anionic ion species (e.g. $Fe(OH)_4^-$ and $Fe(OH)_6^{3-}$) instead of $Fe(OH)_3(s)$ [36, 55, 56].

Ferrate (VI) in aqueous solution occurs in four forms that depend on pH [57-59] as is shown below:



This ferrate (VI) speciation against pH indicates that FeO_4^{2-} is the dominant form in alkaline conditions, and $HFeO_4^-$ predominates in mildly acidic conditions. This explains the instability of FeO_4^{2-} under acidic pH. Therefore, the best performance of ferrate (VI) as an oxidizing agent may correspond to pH of 9.2~10.

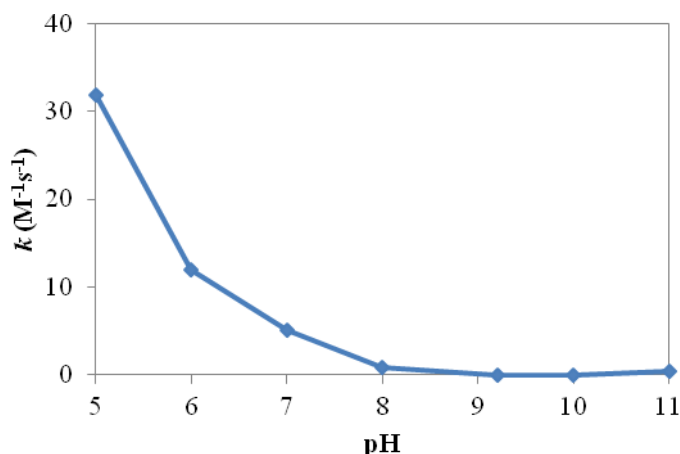


Figure 11. Second order rate constant, k , of ferrate (VI) decay at different pH (initial ferrate (VI) concentration was 1.65 ± 0.01 mM).

4. CONCLUSIONS

The electrochemical synthesis of ferrate (VI) has been investigated using high purity iron anodes in NaOH media. The main factors that affect the electrochemical synthesis of ferrate (VI) have been optimized according to the higher current efficiency and lower energy consumption with desired

amount of ferrate (VI). The electrolyte concentration of 20 M had the best performance. The current density of 1.47 mA/cm² gave the highest current efficiency and the lowest energy consumption. Higher temperatures also affect positively on the formation of ferrate (VI). Ferrate (VI) formation and optimum conditions were confirmed by CV. It was found that the decomposition rate of electrosynthesized ferrate (VI) depends on many factors such as type of electrolyte, initial concentration, temperature, alkalinity, and pH.

ACKNOWLEDGEMENT

The authors gratefully acknowledge the financial support of The Scientific and Technological Research Council of Turkey (TUBITAK).

References

1. M. De Francesco and P. Costamagna, *J. Clean. Prod.*, 12 (2004) 159
2. F. Shen, X. Chen, P. Gao and G. Chen, *Chem. Eng. Sci.*, 58 (2003) 987
3. L. Szpyrkowicz, G. H. Kelsall, S. N. Kaul and M. De Faveri, *Chem. Eng. Sci.*, 56 (2001) 1579
4. J.L. Trinstancho-Reyes, M. Sanchez-Carrillo, R. Sandoval-Jabalera, V.M. Orozco- Carmona, F. Almeraya-Calderón, J.G Chacón-Naval, J. G. Gonzalez-Rodriguez and A. Martínez-Villafañe, *Int. J. Electrochem. Sci.*, 6 (2011) 419.
5. Y. Jung, *Int. J. Electrochem. Sci.*, 8 (2013) 6784.
6. C. C. Arteaga, *Int. J. Electrochem. Sci.*, 7 (2012) 12283.
7. V. K. Sharma, *Environ. Sci. Technol.*, 45 (2010) 645
8. V. K. Sharma, *J. Environ. Manage.*, 92 (2011) 1051
9. Y. Lee and U. V. Gunten, *Water Res.*, 44 (2010) 555
10. V. K. Sharma, M. Sohn, G. A. K. Anquandah and N. Nesnas, *Chemosphere*, 87 (2012) 644
11. G. A. K. Anquandah, V. K. Sharma, V. R. Panditi, P. R. Gardinali, H. Kim and M. A. Oturan, *Chemosphere*, 91 (2013) 105
12. J.Y. Hu, V.K. Sharma, M.L. Tint, Z.B. Zhang and S.L. Ong, *Adv. Asian Environ. Eng.*, 17 (2008) 89
13. J.Q. Jiang, Z. Zhou and O. Pahl, *Sep. Purif. Technol.*, 88 (2012) 95
14. N. Noorhasan, B. Patel and V. K. Sharma, *Water Res.*, 44 (2010) 927
15. J. Q. Jiang, C. Stanford and M. Alsheyab, *Sep. Purif. Technol.*, 32 (2009) 1
16. V. Lescuras-Darrou, F. Lapticque and G. Valentin, *J. App. Electrochem.*, 32 (2002) 57
17. C. Zhang, Z. Liu, F. Wu, L. Lin and F. Qi, *Electrochem. Commun.*, 6 (2004) 1104
18. Z. Ding, C. Yang and Q. Wu, *Electrochim. Acta*, 49 (2004) 3155
19. W. He, J. Wang, C. Yang and J. Zhang, *Electrochim. Acta*, 51 (2006) 1967
20. M. D. Koninck, T. Brousse and D. Belanger, *Electrochim. Acta*, 48 (2003) 1425
21. R. H. Wood, *J. American Chem. Soc.*, 80 (1958) 2038
22. K. Bouzek, I. Rousar, H. Bergmann and K. Hertwig, *J. Electroanal. Chem.*, 425 (1997) 125
23. Z. Macova, K. Bouzek, J. Hives and V. K. Sharma, *Electrochim. Acta*, 54 (2009) 2673
24. L. Nikolic-Bujanovic, M. Cekerevac, M. Vojinovic-Miloradov, A. Jokic and M. Simicic, *J. Ind. Eng. Chem.*, 18 (2012) 1931
25. M. Cekerevac, M. Simicic and L. Nikolic-Bujanovic, *Corros. Sci.*, 64 (2012) 204
26. J. Q. Jiang, N. Graham, C. Andre, G. H. Kelsall and N. Brandon, *Water Res.*, 36 (2002) 4064
27. K. Bouzek and I. Rousar, *J. App. Electrochem.*, 26 (1996) 919
28. K. Bouzek and I. Rousar, *J. App. Electrochem.*, 27 (1997) 679
29. K. Bouzek, M. J. Schmidt and A. A. Wragg, *J. Chem. Technol. Biot.*, 74 (1999) 1188
30. J. Tousek, *Collect. Czech. Chem. Commun.*, 27 (1962) 914
31. M. Alsheyab, J. Q. Jiang and C. Stanford, *Desalination*, 254 (2010) 175

32. M. D. Johnson and K. D. Sharma, *Inorg. Chim. Acta*, 293 (1999) 229
33. G. R. Xu, Y. P. Zhang and G. B. Li, *J. Hazard. Mater.*, 161 (2009) 1299
34. Y. Lee, M. Cho, J. Y. Kim and J. Yoon, *J. Ind. Eng. Chem.*, 10 (2004) 161
35. J. M. Schreyer and L. T. Ockerman, *Analyt. Chem.*, 23 (1951) 1312
36. C. Li, X. Z. Lee and N. Graham, *Chemosphere*, 61 (2005) 537
37. J. D. Carr, P. B. Kelter and A. T. Ericson, *Environ. Sci. Technol.*, 15 (1981) 184
38. H. D. Jia, X. L. Yang, Y. Yang and Y. Gao, *Chin. J. Anal. Chem.*, 27 (1999) 617
39. W. He, J. Wang, H. Shao, J. Zhang and C. N. Cao, *Electrochem. Commun.*, 7 (2005) 607
40. S. Licht, R. Tel-Vered and L. Halperin, *J. Electrochem. Soc.*, 151(1) (2003) 31
41. K. Bouzek, I. Rousar and M. A. Taylor, *J. App. Electrochem.*, 26 (1996) 925
42. H. Vogt, O. Aras and J. Balzer, *Int. J. Heat Mass Tran.*, 47 (2004) 787
43. H. Vogt, *Electrochim. Acta*, 87 (2013) 611
44. M. Alsheyab, J. Q. Jiang and C. Stanford, *J. Chem. Health Safety*, 15 (2008) 16
45. F. Beck, R. Kaus and M. Oberst, *Electrochim. Acta*, 30 (1985) 173
46. K. Bouzek and M. Nejezchleba, *Collect. Czech. Chem. Commun.*, 64 (1999) 2044
47. L. Hrnčiariková, K. Kerekeš, J. Híveš and M. Gál, *Int. J. Electrochem. Sci.*, 8 (2013) 7768.
48. A. Denvir and D. Pletcher, *J. App. Electrochem.*, 26 (1996) 823
49. Z. Xu, J. Wang, H. Shao, Z. Tang and T. Zhang, *Electrochem. Commun.*, 9 (2007) 371
50. G. A. Bailie, K. Bouzek, P. Lukasek, I. Rousar and A. A. Wragg, *J. Chem. Technol. Biot.*, 66 (1996) 35
51. K. A. Walz, J. R. Szczech, A. N. Suyama, W. E. Suyama, L. C. Stoiber, W. A. Zeltner, M. E. Armacanqui and M. A. Anderson, *J. Electrochem. Soc.*, 153(6) (2006) 1102
52. J. Q. Jiang and B. Lloyd, *Water Res.*, 36 (2002) 1397
53. D. Tiwari and S. M. Lee, *J. Environ. Sci.*, 21 (2009) 1347
54. J. K. Yang, D. Tiwari, M. R. Yu, L. Pachuau and S. M. Lee, *Environ. Technol.*, 31 (2010) 791
55. E. L. Yang, J. J. Shi and H. C. Liang, *Electrochim. Acta*, 63 (2012) 369
56. V. K. Sharma, R. A. Rendon, F. J. Millero and F. G. Vasquez, *Mar. Chem.*, 70 (2000) 235
57. N. Graham, C. C. Jiang, X. Z. Li, J. Q. Jiang and J. Ma, *Chemosphere*, 56 (2004) 949
58. S. Licht, V. Naschitz, L. Halperin, N. Halperin, L. Lin, J. J. Chen, S. Ghosh and B. Liu, *J. Power Sources*, 101 (2001) 167
59. V. K. Sharma, *Adv. Environ. Res.*, 6 (2002) 143